PROCEEDINGS OF SPIE

SPIEDigitalLibrary.org/conference-proceedings-of-spie

Spectroscopy of erbium-doped potassium double tungstate waveguides

Sergio Vázquez-Córdova, Shanmugam Aravazhi, Christos Grivas, Alexander Heuer, Christian Kränkel, et al.

Sergio A. Vázquez-Córdova, Shanmugam Aravazhi, Christos Grivas, Alexander M. Heuer, Christian Kränkel, Yean-Sheng Yong, Sonia M. García-Blanco, Jennifer L. Herek, Markus Pollnau, "Spectroscopy of erbium-doped potassium double tungstate waveguides," Proc. SPIE 10106, Integrated Optics: Devices, Materials, and Technologies XXI, 1010604 (16 February 2017); doi: 10.1117/12.2252488

SPIE.

Event: SPIE OPTO, 2017, San Francisco, California, United States

Spectroscopy of erbium-doped potassium double tungstate waveguides

Sergio A. Vázquez-Córdova,[1,*] Shanmugam Aravazhi,[2] Christos Grivas,[3] Alexander M. Heuer,[4] Christian Kränkel,[4] Yean-Sheng Yong,[1] Sonia M. García-Blanco,[1] Jennifer L. Herek,[1] and Markus Pollnau[2,5]

[1]Optical Sciences, MESA+ Institute, University of Twente,
P.O. Box 217, 7500 AE Enschede, The Netherlands

[2]Integrated Optical Microsystems, MESA+ Institute, University of Twente,
P.O. Box 217, 7500 AE Enschede, The Netherlands

[3]School of Physics and Astronomy, University of Southampton, Southampton SO17 1BJ, UK

[4]Institute of Laser-Physics, University of Hamburg,
Luruper Chaussee 149, 22761 Hamburg, Germany

[5]Department of Materials and Nano Physics, KTH–Royal Institute of Technology,
Isafjordsgatan 22-24, 16440 Kista, Sweden

*s.a.vazquezcordova-1@utwente.nl

ABSTRACT

We report the spectroscopy of crystalline waveguide amplifiers operating in the telecom C-band. Thin films of erbium-doped gadolinium lutetium potassium double tungstate, $KGd_xLu_yEr_{1-x-y}(WO_4)_2$, are grown by liquid- phase epitaxy onto undoped potassium yttrium double tungstate (KYW) substrates and micro-structured by Ar^+- beam etching. Channel waveguides with erbium concentrations between 0.45–6.35 × 10^{20} cm^{-3} are characterized. The transition cross-sections of interest are estimated. The effect of energy-transfer up-conversion (ETU) is experimentally investigated. Microscopic and macroscopic ETU parameters are extracted from a simultaneous analysis of 20 decay curves of luminescence on the transition $^4I_{13/2} \rightarrow {}^4I_{15/2}$. The correlation between ETU and the doping concentration is studied. Pump excited-state absorption (ESA) on the transition $^4I_{11/2} \rightarrow {}^4F_{7/2}$ is investigated via a direct ESA measurement using a double-modulation pump-probe technique. The effect of ESA is studied for different pump wavelengths. The pump wavelength of 984.5 nm is found to be favorable for the complete range of erbium concentrations.

Keywords: Rare-earth doped, waveguide amplifiers, EDWA, crystalline waveguides

1. INTRODUCTION

Amorphous and crystalline rare-earth-doped materials are of special interest for amplifiers [1–6] and lasers [1,7–9]. In particular, erbium-doped materials are appealing for signal regeneration in telecommunications [1], where the erbium-doped fiber amplifier (EDFA) has been extensively used in boosting optical signals in the C-band (1.525–1.565 μm). With the rapid development of optical integrated circuits (OIC) [10], there is a need of an amplifier with similar properties as the EDFA, yet down-scalable to millimeter dimensions. Electrically pumped semiconductor optical amplifiers (SOA) have been widely employed as active building blocks in OIC [11]. Intrinsic limitations of these devices are not observed in erbium-doped amplifiers. High transmission speeds are possible in Er^{3+}-doped materials [12] due to the long excited-state lifetimes. Amplification of wavelength-division-multiplexed signals, which can be fully exploited in EDFA, in SOAs leads to channel cross-talk and deterioration of the signals [11]. Additionally, low refractive index changes as a consequence of excitation are observed in rare-earth-doped materials [13], in contrast to significant refractive index changes induced by electron-hole pairs in SOAs. Moreover, SOAs usually require active temperature control for heat management and device stability, in comparison with erbium-doped amplifiers where only a slight influence of temperature on its performance is observed [6].

Incorporation of a higher number of erbium ions per unit volume is required in Er^{3+}-doped waveguide amplifiers to achieve similar performance as EDFAs at a shorter scale. Nonetheless, detrimental processes such as ETU and concentration quenching become stronger with increasing Er^{3+} concentration, thereby limiting the maximum gain per

Integrated Optics: Devices, Materials, and Technologies XXI, edited by Sonia M. García-Blanco, Gualtiero Nunzi Conti, Proc. of SPIE Vol. 10106, 1010604 · © 2017 SPIE
CCC code: 0277-786X/17/$18 · doi: 10.1117/12.2252488

unit length [14]. Despite this limitation, good performance has been achieved in long spiral waveguide amplifiers, where 20 dB of internal net gain was demonstrated in amorphous aluminum oxide with $N_d = 1.9 \times 10^{20}$ cm^{-3} [6].

Reduction of the influence of energy-transfer processes by increasing the Er-Er distance, using a multilayer approach by atomic layer deposition, has been recently proposed [15]. However, a simpler, less expensive and higher-throughput solution is to incorporate Er ions in a crystalline matrix, such as potassium double tungstates, where the inter-ionic distance is larger compared to other host materials and potentially limits the energy-transfer processes enabling higher doping concentrations [16,17]. In addition, Er^{3+} ions in potassium double tungstates exhibit one of the highest transition cross-sections with a broad band emission. The peak transition cross-section near 1.53 μm is 4 times larger when compared to a-Al_2O_3:Er^{3+} [18,19]. In addition, the peak of the ground-state absorption (GSA) to the $^4I_{11/2}$ level is almost 6 times higher, allowing for more efficient pumping [20, 21]. Furthermore, the high refractive indices (~2) of potassium double tungstates could allow for high-contrast waveguides and potentially dense integration of optical functions on a chip.

Here we present a spectroscopic study of erbium-doped gadolinium lutetium potassium double tungstate waveguide amplifiers, which allows the understanding of the amplification process of signals with wavelengths around 1.55 μm.

2. WAVEGUIDE DESIGN AND FABRICATION

All rare-earth doped potassium double tungstates crystalize in the same monoclinic centrosymmetric space group $C_{2/c}$, albeit with different lattice parameters [23–25] and refractive indices [26–28]. The difference in refractive indices enables the growth of light-guiding layers due to the refractive index contrast achieved between two different potassium rare-earth double tungstates. However, due to the difference in lattice parameters engineering of the layer composition is required [22]. Crystalline layers of erbium-doped potassium double tungstates were grown from solution onto b-oriented undoped $KY(WO_4)_2$ substrates by liquid-phase epitaxy (LPE) [22]. Five samples with different Er^{3+} concentrations of 0.75, 1.5, 3, 6, and 10 at. % (0.48, 0.95, 1.9, 3.81, and 6.36×10^{20} cm^{-3}, respectively) lattice matched by appropriate Gd^{3+} and Lu^{3+} concentrations were produced.

Planar guiding layers were prepared after LPE by lapping and polishing parallel to the substrate plane until the desired thickness was achieved. Standard lithography techniques were used to define the channel waveguides. Rib-channel waveguides were micro-structured by Ar^+ etching [29] parallel to the N_g axis in the N_m–N_g plane of the crystalline layer, hence the optical modes can propagate with a polarization of either $E||N_m$ or $E||N_p$. In this study the polarization $E||N_m$ was employed. A range of channel widths and thicknesses from 3–8 μm were fabricated. The rib height of ~1.5 μm was fixed by limitations of the etching process, resulting in fundamental-mode profiles with dimensions < 10 × 10 μm^2.

3. EXPERIMENTAL TECHNIQUES AND RESULTS

Polarized luminescence spectra on the $^4I_{13/2} \rightarrow {}^4I_{15/2}$ and the $^4I_{11/2} \rightarrow {}^4I_{15/2}$ transitions were recorded parallel to the three principal axes after pumping at 984.5 nm and 800 nm, respectively. A continuous-wave (CW) Ti:Sapphire laser was employed as a pump source during the measurements. The radiative lifetime [30] and the luminescence spectra were used to determine the transition cross-sections.

Luminescence-decay curves on the $^4I_{13/2} \rightarrow {}^4I_{15/2}$ transition were measured after direct excitation using a fiber-Bragg-grating-stabilized diode laser (1480 nm) modulated using an external function generator. The laser diode was modulated at 20 Hz by a square wave with 50% duty cycle. Four different initial excitation densities were achieved by varying the maximum pump power during the ON-part of the cycle. The initial incident pump power was ~25 mW, which was doubled every subsequent pumping step. The pump light was coupled to the waveguides by direct butt coupling from a single-mode fiber to the channel waveguide. Luminescence on the transition $^4I_{13/2} \rightarrow {}^4I_{15/2}$ was collected using a multimode light-guide fiber placed on top of the excited waveguide. A monochromator, whose wavelength was centered at 1535 nm, was employed to remove the scattered pump light, and the signal was detected by an InGaAs photodiode. The photo-generated current was amplified (FEMTO DHPCA-100) and recorded with an oscilloscope (HP Infinium 54845A). The oscilloscope was synchronized with the function generator driving the laser diode. A schematic diagram of the setup is shown in Fig. 1.

Four luminescence decay curves at different initial excitation densities for each of the 5 samples with different doping concentrations were recorded. Non-exponential decay curves were recorded due to the presence of ETU ($^4I_{13/2}$, $^4I_{13/2}$) →

($^4I_{15/2}$, $^4I_{9/2}$), especially at the 3 highest doping concentrations. A total of 20 decay curves were studied using the approach presented in [14, 31]. A modified Zubenko equation [14]

$$N_1(t) = \frac{N_1(0)e^{-t/\tau_1}}{1 + N_1(0)\frac{\pi^2}{3}\tau_1\sqrt{C_{DA}\tau_0^{-1}}\left\{\sqrt{1+\tau_0\tau_1^{-1}}\,\mathrm{erf}\left[\sqrt{t\left(\tau_0^{-1}+\tau_1^{-1}\right)}\right] - e^{-t/\tau_1}\,\mathrm{erf}\left(\sqrt{t\tau_0^{-1}}\right)\right\}} \quad (1)$$

was fitted to the 20 normalized luminescence decay curves by minimizing the residual error of all fittings, since the luminescence intensity is proportional to the density of ions in the excited state $N_1(t)$. $N_1(0)$ is the initial excitation density in the $^4I_{13/2}$ level, τ_1 is the intrinsic luminescence lifetime of the $^4I_{13/2}$ level (~3 ms), determined from the exponential decay of the sample with the lowest doping concentration, C_{DA} is the donor-acceptor micro parameter characteristic of the ETU process, τ_0 is the most probable migration time, related to the migration micro-parameter C_{DD} by $1/\tau_0 = C_{DD}N_d^2$ [14]. Only C_{DD} and C_{DA} were set as free parameters during the fitting, whose determination allows us to evaluate the macroscopic ETU parameter by $W_{ETU} = \pi^2/3(C_{DD}C_{DA})^{1/2}N_d$. Figure 2 presents the ETU coefficient for the range of Er^{3+} concentrations studied.

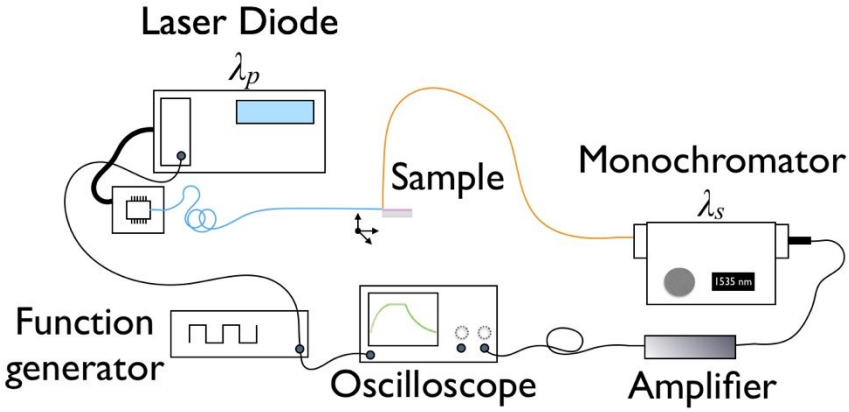

Figure 1. Schematic of the luminescence decay setup.

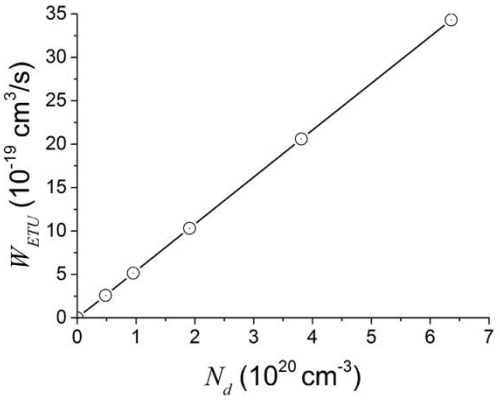

Figure 2. Macroscopic ETU coefficient determined for the range of doping concentrations studied.

Laser diodes at $\lambda_P \approx 980$ nm are commonly employed for pumping Er^{3+}-doped amplifiers since the photon energy overlaps with the energy difference between the ground state and the $^4I_{11/2}$ level, which triggers the transition $^4I_{15/2} \rightarrow {}^4I_{11/2}$ by the absorption of a pump photon. Nevertheless, the pump-photon energy usually also spectrally overlaps with the transition $^4I_{11/2} \rightarrow {}^4F_{7/2}$, enabling pump ESA when the population of the $^4I_{11/2}$ level becomes significant. This wavelength-dependent process indirectly decreases the excitation of the $^4I_{13/2}$ amplifier level, additionally to the ETU process, which directly reduces the $^4I_{13/2}$ population. Nevertheless, with knowledge of the ESA spectra it is possible to reduce the impact of ESA on the amplifier performance.

ESA can be directly measured using a pump-probe technique where a double modulation, of the pump and the signal, allows for a very sensitive detection of signal intensity [32]. A setup similar to the one presented in [32] was used and its schematic is presented in Fig. 3. The beam from a Ti:Sapphire laser modulated at ~11 Hz was launched into the waveguide using a microscope objective in counter-propagation direction to the signal. The output of a white-light source, used as the signal, was polarized and coupled into the channel waveguide by use of a microscope objective. The signal was modulated as well, but at higher frequency (~1 kHz), and the transmitted signal was dispersed by a monochromator and detected by a silicon detector. The electrical output of the detector was amplified by a lock-in amplifier synchronous with the modulated signal, while a second lock-in amplifier was used to detect signal variations induced by the pump, thus this amplifier had the reference frequency of the pump.

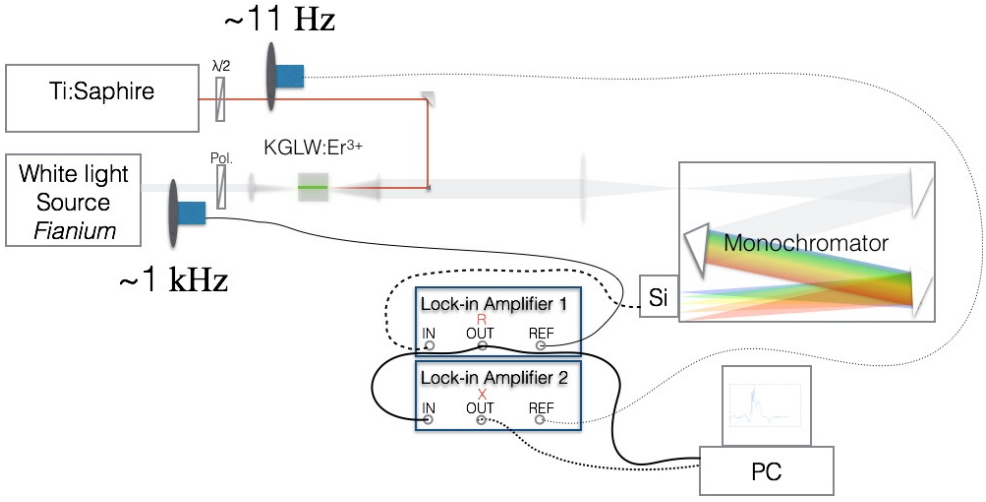

Figure 3. Schematic diagram of the double-modulation pump-probe setup.

ESA cross-sections and, for comparison, the GSA cross-sections are shown in Fig. 4, both for $E||N_m$. The analysis of the ESA cross-sections proofed difficult because of slightly different resolution of the ESA, GSA and emission spectra, and especially the region around 974 nm should not be over-interpreted. Nevertheless, the peak of the GSA cross-sections at 979 nm does not coincide with the peak of the ESA cross-sections. In addition, the ESA cross-section at 984.5 nm is much lower of that at the peak GSA cross-section, whereas the difference in GSA cross-section between these two wavelengths is rather small.

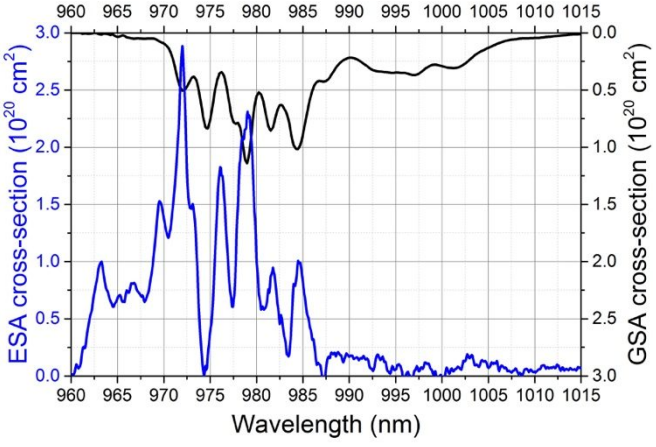

Figure 4. ESA cross-sections on the $^4I_{11/2} \rightarrow {}^4F_{7/2}$ transition (blue line) and GSA cross sections on the $^4I_{15/2} \rightarrow {}^4I_{11/2}$ transition (black line).

Based on the above findings the selection of the pump wavelength to be 984.5 nm seems favorable to maximize GSA while reducing ESA.

4. SUMMARY

Rib-channel waveguides were patterned onto Er^{3+}-doped potassium gadolinium lutetium double tungstate layers grown onto undoped KYW substrates. A study of the luminescence decay curves from the $^4I_{13/2}$ level was used for the determination of the intrinsic lifetime and the macroscopic ETU parameter for the range ($0.48–6.4 \times 10^{20}$ cm^{-3}) of Er^{3+} concentrations. ESA cross-sections from the $^4I_{11/2} \rightarrow {}^4F_{7/2}$ transition were determined using a double-modulation pump-probe technique. A good pump wavelength was determined to be 984.5 nm where the ESA is substantially reduced while the GSA remains barely affected as compared to the peak GSA. Both, ETU parameters and ESA cross-sections required for simulating the performance of a channel waveguide amplifier employing a set of rate equations.

REFERENCES

[1] Bradley, J.D.B., and Pollnau, M., "Erbium-doped integrated waveguide amplifiers and lasers," Laser Photonics Rev. 5(3), 368–403 (2011).

[2] Geskus, D., Aravazhi, S., García-Blanco, S.M., and Pollnau, M., "Giant optical gain in a rare-earth-ion-doped microstructure," Adv. Mater. 24(10), OP19–OP22 (2012).

[3] Yang, J., Diemeer, M.B.J., Geskus, D., Sengo, G., Pollnau, M., and Driessen, A., "Neodymium-complex-doped photodefined polymer channel waveguide amplifiers," Opt. Lett. 34(4), 473–475 (2009).

[4] Wörhoff, K., Bradley, J.D.B., Ay, F., Geskus, D., Blauwendraat, T.P., and Pollnau, M., "Reliable low-cost fabrication of low-loss $Al_2O_3:Er^{3+}$ waveguides with 5.4-dB optical gain," IEEE J. Quantum Electron. 45(5), 454–461 (2009).

[5] Yang, J., Dalfsen, K., Wörhoff, K., Ay, F., and Pollnau, M., "High-gain $Al_2O_3:Nd^{3+}$ channel waveguide amplifiers at 880 nm, 1060 nm, and 1330 nm," Appl. Phys. B 101(1–2), 119–127 (2010).

[6] Vázquez-Córdova, S.A., Dijkstra, M., Bernhardi, E.H., Ay, F., Wörhoff, K., Herek, J.L., García-Blanco, S.M., and Pollnau, M., "Erbium-doped spiral amplifiers with 20 dB of net gain on silicon," Opt. Express 22(21), 25993–26004 (2014).

[7] Bernhardi, E.H., van Wolferen, H.A.G.M., Agazzi, L., Khan, M.R.H., Roeloffzen, C.G.H., Wörhoff, K., Pollnau, M., and de Ridder, R.M., "Ultra-narrow-linewidth, single-frequency distributed feedback waveguide laser in $Al_2O_3:Er^{3+}$ on silicon," Opt. Lett. 35(14), 2394–2396 (2010).

[8] van Dalfsen, K., Aravazhi, S., Geskus, D., Wörhoff, K., and Pollnau, M., "Efficient $KY_{1-x-y}Gd_xLu_y(WO_4)_2:Tm^{3+}$ channel waveguide lasers," Opt. Express 19(6), 5277–5282 (2011).

[9] van Dalfsen, K., Aravazhi, S., Grivas, C., García-Blanco, S.M., and Pollnau, M., "Thulium channel waveguide laser with 1.6 W of output power and ~80% slope efficiency," Opt. Lett. 39(15), 4380–4383 (2014).

[10] Kaminow, I.P., "Optical integrated circuits: A personal perspective," J. Lightwave Technol. 26(9), 994–1004 (2008).

[11] Spiekman, L.H., "Semiconductor Optical Amplifiers," in *Optical Fiber Telecommunication* IV-A Fourth Edition, Kaminow, I.P., and Li, T., Eds. (Academic Press, San Diego, CA, USA, 2002), 699–731.

[12] Bradley, J.D.B., Costa e Silva, M., Gay, M., Bramerie, L., Driessen, A., Wörhoff, K., Simon, J.-C., and Pollnau, M., "170 Gbit/s transmission in an erbium-doped waveguide amplifier on silicon," Opt. Express 17(24), 22201–22208 (2009).

[13] Soulard, R., Zinoviev, A., Doualan, J.L., Ivakin, E., Antipov, O., and Moncorgé, R., "Detailed characterization of pump-induced refractive index changes observed in $Nd:YVO_4$, $Nd:GdVO_4$ and Nd:KGW," Opt. Express 18(2), 1553–1568 (2010).

[14] Agazzi, L., Wörhoff, K., and Pollnau, M., "Energy-transfer-upconversion models, their applicability and breakdown in the presence of spectroscopically distinct ion classes: a case study in amorphous $Al_2O_3:Er^{3+}$," J. Phys. Chem. C 117(13), 6759–6776 (2013).

[15] Rönn, J., Karvonen, L., Kauppinen, C., Perros, A.P., Peyghambarian, N., Lipsanen, H., Säynätjoki, A., and Sun, Z., "Atomic layer engineering of Er-ion distribution in highly doped $Er:Al_2O_3$ for photoluminescence enhancement," ACS Photonics 3(11), 2040–2048 (2016).

[16] Pujol, M.C., Mateos, X., Solé, R., Massons, J., Gavalda, J., Solans, X., Díaz, F., and Aguiló, M., "Structure, crystal growth and physical anisotropy of $KYb(WO_4)_2$, a new laser matrix," J. Appl. Crystallogr. 35, 108–112 (2002).

[17] Krygin, I.M., Prokhorov, A.D., D'yakonov, V.P., Borowiec, M.T., and Szymczak, H., "Spin-spin interaction of Dy^{3+} ions in $KY(WO_4)_2$," Phys. Solid State 44(8), 1587–1596 (2002).
[18] Kuleshov, N.V., Lagatsky, A.A., Podlipensky, A.V., Mikhailov, V.P., Kornienko, A.A., Dunina, E.B., Hartung, S., and Huber, G., "Fluorescence dynamics, excited-state absorption, and stimulated emission of Er^{3+} in $KY(WO_4)_2$," J. Opt. Soc. Am. B 15(3), 1205–1212 (1998).
[19] Bradley, J.D.B., Agazzi, L., Geskus, D., Ay, F., Wörhoff, K., and Pollnau, M., "Gain bandwidth of 80 nm and 2 dB/cm peak gain in Al_2O_3:Er^{3+} optical amplifiers on silicon," J. Opt. Soc. Am. B 27(2), 187–196 (2010).
[20] Rico, M., Pujol, M.C., Díaz, F., and Zaldo, C., "Green up-conversion of Er^{3+} in $KGd(WO_4)_2$ crystals. Effects of sample orientation and erbium concentration," Appl. Phys. B 72(2), 157–162 (2001).
[21] Agazzi, L., Wörhoff, K., Kahn, A., Fechner, M., Huber, G., and Pollnau, M., "Spectroscopy of upper energy levels in an Er^{3+}-doped amorphous oxide," J. Opt. Soc. Am. B 30(3), 663–667 (2013).
[22] Aravazhi, S., Geskus, D., van Dalfsen, K., Vázquez-Córdova, S.A., Grivas, C., Griebner, U., García-Blanco, S.M., and Pollnau, M., "Engineering lattice matching, doping level, and optical properties of $KY(WO_4)_2$:Gd, Lu, Yb layers for a cladding-side-pumped channel waveguide laser," Appl. Phys. B 111(3), 433–446 (2013).
[23] Borisov, S.V., and Klevtsova, R.F., "Crystal structure of $KY(WO_4)_2$," Sov. Phys. Crystallogr. 13(3), 420–421 (1968). (Transl.: Kristallografiya 13(3), 517–519 (1968))
[24] Klevtsov, P.V., and Kozeeva, L.P., "Synthesis X-ray and thermographic study of potassium rare-earth tungstates, $KLn(WO_4)_2$, Ln = rare- earth elements," Sov. Phys. Doklady 14, 185–187 (1969). (Transl.: Doklady Akademii Nauk SSSR 185(3), 571–574 (1969))
[25] Pujol, M.C., Aguiló, M., Díaz, F., and Zaldo, C., "Growth and characterisation of monoclinic $KGd_{1-x}RE_x(WO_4)_2$ single crystals," Opt. Mater. 13(1), 33–40 (1999).
[26] Pujol, M.C., Rico, M., Zaldo, C., Solé, R., Nikolov, V., Solans, X., Aguiló, M., and Díaz, F., "Crystalline structure and optical spectroscopy of Er^{3+}-doped $KGd(WO_4)_2$ single crystals," Appl. Phys. B 68(2), 187–197 (1999).
[27] Kaminskii, A.A., Gruber, J.B., Bagaev, S.N., Ueda, K., Hömmerich, U., Seo, J.T., Temple, D., Zandi, B., Kornienko, A.A., Dunina, E. B., Pavlyuk, A.A., Klevtsova, R.F. and Kuznetsov. F.A., "Optical spectroscopy and visible stimulated emission of Dy^{3+} ions in monoclinic α-$KY(WO_4)_2$ and α-$KGd(WO_4)_2$ crystals," Phys. Rev. B 65(12), 125108 (2002).
[28] Pujol, M.C., Mateos, X., Aznar, A., Solans, X., Suriñach, S., Massons, J., Díaz, F., and Aguiló, M., "Structural redetermination, thermal expansion and refractive indices of $KLu(WO_4)_2$," J. Appl. Crystallogr. 39(2), 230–236 (2006).
[29] Grivas, C., Shepherd, D.P., May-Smith, T.C., Eason, R.W., Pollnau, M., Crunteanu, A., and Jelinek, M., "Performance of Ar^+-milled Ti:Sapphire rib waveguides as single transverse-mode broadband fluorescence sources," IEEE J. Quantum Electron. 39(3), 501–507 (2003).
[30] Martínez de Mendívil, J., Lifante, G., Pujol, M.C., Aguiló, M., Díaz, F., and Cantelar, E., "Judd-Ofelt analysis and transition probabilities of Er^{3+} doped $KY_{1-x-y}Gd_xLu_y(WO_4)_2$ crystals," J. Lumin. 165, 153–158 (2015).
[31] Zubenko, D.A., Noginov, M.A., Smirnov, V.A., and Shcherbakov, I.A., "Different mechanisms of nonlinear quenching of luminescence," Phys. Rev. B 55(14), 8881–8886 (1997).
[32] Koetke, J., and Huber, G., "Infrared excited-state absorption and stimulated-emission cross sections of Er^{3+}-doped crystals," Appl. Phys. B 61(2), 151–158 (1995).